

A novel approach to Under-Actuated Control of Fluidic Systems

Antonio Di Lallo^{1,2,3}, Manuel Catalano³, Manolo Garabini¹,
Giorgio Grioli³, Marco Gabiccini^{1,2} and Antonio Bicchi^{1,3}

Abstract—Thanks to the growing interest in soft robotics, hydropneumatics and inflatable system dynamics are attracting renewed attention from the scientific community. Typical fluidic systems are composed of several chambers and require a complex and bulky network of active components for their control. This paper presents a novel approach to fluidic actuation, which consists in the co-design of both the mechanical parameters of the system and of custom input signals, to enable the elicitation of different behaviors of the system with fewer control components. The principle is presented in theory and simulation and then experimentally validated through the application to a case study, an in-pipe inchworm-like robot. It is shown that it is possible to obtain forward and backward movements by modulating a unique input.

I. INTRODUCTION

In the last years, inspired by biological systems, robotics has been pushing the application of soft robot systems, either fabricated in continuous deformable materials (continuous soft robots) [1], [2], or using lumped passive visco-elastic elements in their structure (variable impedance robots) [3], [4]. The use of soft materials in robots allows for extremely lightweight and economic structures. Among soft-bodied robots, a considerable category is represented by inflatable robots, composed mostly of pressurized air chambers. Typically they require one or two pneumatic lines for each independent chamber and just as much as equal set of active control valves.

Several fields see the possibility of the application of soft inflatable robots, some of them are already on the market. Among these we can enumerate all applications that revolve around safe PHRI (Physical Human-Robot Interaction), from toy-like systems for the study of human behavior and emotions [5], to portable air-bags [6], [7] and emergency lifters for the elderly [8] - already at the commercial level - to adaptive soft grippers and hands [9], [10], [11], to many sorts of bio-mimetic [12], [13] or bio-inspired [14], [15] robots, including e.g. worm robots, used for pipe inspections, maintenance and diagnostics [16], [17], [18].

As mentioned, most of robots based on fluidic actuation are controlled through open-loop valve sequencing. It is the case of the multi-gait quadrupedal soft robot presented in [19], that uses a network of pneumatic channels for each limb plus one for the spine of the robot. Some recent work address



Fig. 1. 3D CAD rendering of the realized inchworm prototype.

the challenge of reducing valve complexity, by designing simple passive valves which can be selectively activated through deliberate modulation of the input pressure [20]. As actuation of the valves is removed, this method can be seen as a form of under-actuation applied to inflatable structures. This goal is pursued also by [21] where it is presented an inchworm-like micro robot for pipe inspection that is able to move forward by using only one pneumatic line. Its operating principle is based on the regulation of the air flow between chambers through different-sized micro holes drilled in the separation plates. In fact, an inchworm-like moving mechanism has at least three separate chambers to integrate the rear clamp, the middle elongation module and the front clamp. A step further is taken in [22], where the authors exploit the close analogy between electrical and fluidic circuits to control an entirely soft untethered octobot through an integrated microfluidic logic. These works suggest the opportunity of simplifying the system by reducing the number of pipes and valves needed to operate it. The role of active control components can be transferred to a suitable design of the system. In particular, by purportedly shaping the mechanical stiffness and damping, it is possible to associate different behaviors to different pressure inputs.

In this paper we present a method to design the system dynamics and the pressure profile to accomplish the aforementioned task. In Sec. II the general problem is defined, whose solution is approached in Sec. III. Sec. IV proposes an application of the discussed principle to a particular use case, consisting in an inchworm prototype for pipe inspection (see Fig. 1). Conceptual and mechanical designs are exposed in Secs. IV-A and IV-B respectively. Sec. V contains tests executed on the experimental setup, whose results are discussed in Sec. VI; finally conclusions and

*This work was supported by the European Commission project (Horizon 2020 research program) SOMA (no.645599)

¹Research Center “E. Piaggio”, Univ. of Pisa, Italy.

²Dept. of Civil and Industrial Eng. (DICI) of the Univ. of Pisa, Italy

³Soft Robotics for Human Cooperation and Rehabilitation Lab, Istituto Italiano di Tecnologia (IIT), Genoa, Italy

Correspond to: antonio.dilallo@ing.unipi.it

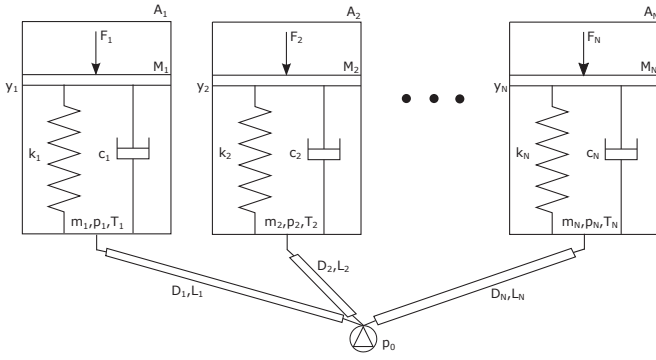


Fig. 2. Schematic representation of a fluidic network with multiple chambers connected in parallel to the same input source. Each chamber is modeled as a mass-spring-damper system.

future work are presented in Sec. VII.

II. PROBLEM DEFINITION

Usually, soft fluidic systems consist of multiple independent chambers individually controlled through a complex network of pipes and active valves. This allows to easily obtain a large variety of movements, which is a desirable property for several applications. Some examples include e.g. hands, where the order of the fingers closing can yield different grasping patterns (see e.g. [23]), or personal lifters, as that in [8], which could adapt their lifting pattern to the shape and position of the person. Another meaningful example, analyzed in sec.IV, is that of pipe-inspection inch-worm robots. All these systems implement different functions mostly thanks to the possibility of inflating/deflating their chambers in different sequences.

Common control techniques result very flexible in accomplishing this, but have the drawback of making the system heavier and bulkier. Our aim is the simplification of the pipe and valve robot actuation network to obtain, in principle with just one single input, different behaviors in the robot.

Model the robot with a pneumatic network composed of N -inflatable chambers, connected in parallel to the pressure source, as shown in Fig. 2. Each chamber is modeled as a piston with a finite stroke, coupled to a spring and a damper, simulating both the equivalent mechanical properties of the chamber and of the connected robot structure. Assuming air as an ideal gas and flow laminar, we can write the dynamics of the system governed by the equations of motion of the pistons and by the mass and energy balances of the air flow.

Each chamber can be described through the following system of nonlinear differential equations [24]:

$$\begin{cases} \dot{m}_i = \frac{p_0 - p_i}{Z_i} & (1) \\ \ddot{y}_i = \frac{1}{M_i} ((p_i - p_{\text{atm}})A_i - F_i - k_i(y_i - l_{ri}) - c_i\dot{y}_i) & (2) \\ \dot{p}_i = \frac{R}{c_v A_i y_i} \left(\dot{m}_i c_p T_{\text{atm}} - \frac{c_p}{R} A_i p_i \dot{y}_i + k_w S_i (T_i - T_{\text{atm}}) \right) & (3) \\ T_i = \frac{p_i A_i y_i}{m_i R} & (4) \end{cases}$$

TABLE I
LIST OF SYMBOLS

Symbol	Description
A	piston area
c	damping coefficient
c_p	heat capacity at constant pressure
c_v	heat capacity at constant volume
D	diameter of the duct
F	external force
k	stiffness
k_w	convective heat transfer coefficient
L	length of the duct
l_r	rest length of the spring
m	mass of the air in the piston
M	mass of the piston
μ	dynamic viscosity of the air
p	absolute pressure
p_0	supply pressure
p_{atm}	atmospheric pressure
R	specific gas constant
ρ	density of the air
S	external surface of the piston
T	temperature
T_{atm}	atmospheric temperature
y	piston height
Z	ratio between pressure drops and flow rate

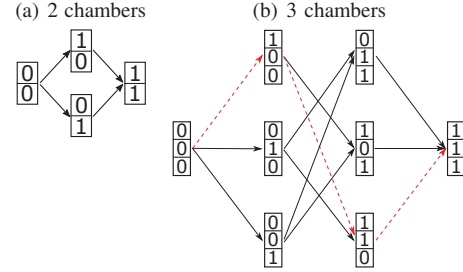


Fig. 3. Possible states configurations and behaviors for two systems. Column vectors of 0s and 1s correspond to system deflation/inflation states, arrows correspond to different inflation actions. Left panel corresponds to a 2-chamber system, while right panel to a 3-chamber one. A particular behavior is highlighted in red dashed line.

where

$$Z_i = \frac{32\mu L_i}{\pi \rho_i D_i^4} \quad (5)$$

$$\rho_i = \frac{m_i}{A_i y_i} \quad (6)$$

$$S_i = y_i \sqrt{4\pi A_i} \quad (7)$$

The definition of symbols is reported in Tab. I.

Given a chamber a , we describe its state as fully inflated ($a = 1$) or deflated ($a = 0$). Consequently, the state of the global system can be described by a vector of N binary digits. We define a behavior each possible sequence of inflation (or deflation) of the different chambers. Fig. 3 illustrates e.g. the sets of all inflation behaviors for two systems with two and three chambers respectively. Each oriented path, from the leftmost state to the rightmost state, along the arrows indicates a possible behavior (simultaneous inflations are neglected for brevity). The left example has just two possible behaviors, while the right one, with three chambers, has six.

Our design objective is, given a subset of n possible behaviors, to determine the control input $p(t)$ and the design

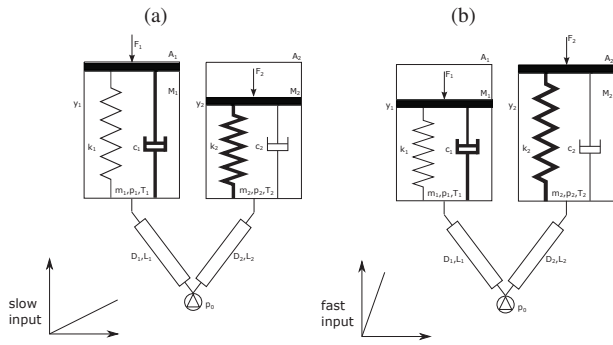


Fig. 4. A fluidic network as those described in sec. II, subjected to two different inputs. The right chamber has higher stiffness than left chamber, while left chamber has higher damping than the right one (i.e. the reverse). For a slow inputs (a) the chamber on the right inflates first, while for faster inputs (b) the one on the left is faster.

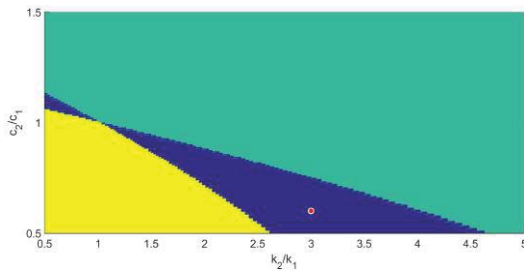


Fig. 5. Behaviors of the two chambers, as a function of the ratios of stiffness k_2/k_1 and of damping c_2/c_1 . Regions in blue indicate that different inputs produce different behaviors in terms of order of inflation. Yellow or green areas denote the regions where chamber 1 or 2, respectively, always inflates first. Blue area is our design space.

of the mechanical parameters of the system, such that all the n behaviors can be achieved.

III. KEY IDEA

For the sake of simplicity, we consider a system composed of two inflatable chambers only, connected in parallel to the same pressure source. The key idea is that by playing on the speed of inflation it is possible to render the dynamic response of the spring dominant over the effect of the damper or vice-versa. When pressure grows quickly damping plays the greatest role, while at low pressure gradients stiffness dominates. A sketch of this idea is shown in Fig. 4.

Assume that the stiffness and the damping of the two chambers can be designed freely. The goal of the task is to determine the mechanical parameters of the two chambers and two pressure profiles such that both inflation sequences are possible.

By simulating the system, it is possible to identify the values of the mechanical parameters for which the intended behavior manifests. Fig. 5 shows the results of such a simulation campaign, highlighting the set of mechanical parameters that satisfy our specifications.

As an example, Fig. 6 shows the behavior of the system corresponding to the red dot in Fig. 5 when three different pressure profiles are applied. Chamber 2 is 0.6 times less damped and 3 times stiffer than chamber 1. No external

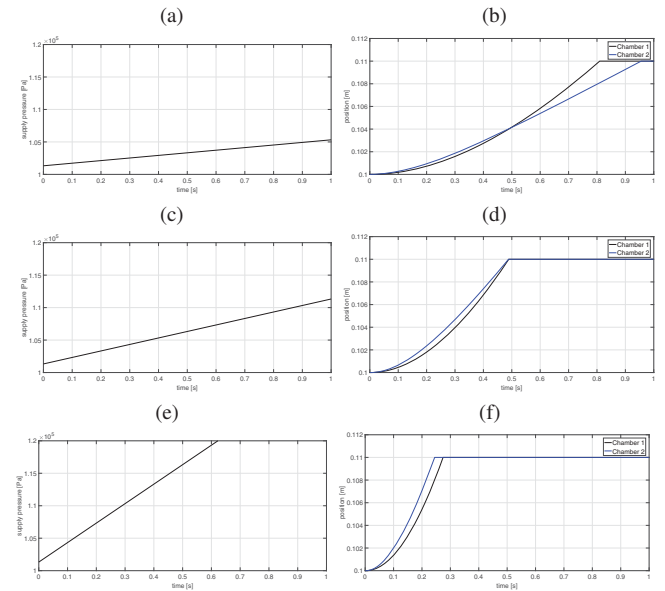


Fig. 6. Evolution of pistons position with respect to different supply pressure gradients.



Fig. 7. Illustration of a possible use case

forces are acting on the chambers, except for the end-stroke limits. It is possible to notice how the steepest pressure profile lets chamber 1 inflate before chamber 2, while the middle pressure profile lets the two chambers inflate at the same time. Finally, the slowest pressure ramp lets chamber 2 inflate before chamber 1.

Fig. 6 highlights also one possible drawback of the proposed technique, the drawback is that the duration of the inflation itself can not be made independent from the desired behavior. While this is an important aspect to keep in mind when applying this design method, it doesn't represent a major problem in non-time-critic applications.

IV. CASE STUDY

A classical application of inflatable systems is that of inchworm robots (see Fig. 7), which due to their shape and operational mechanism are good for pipe maintenance and diagnostics [16], [17], [18]. Internal inspections can be very useful to identify preliminary traces of damage and evoke maintenance before the damage becomes larger and threatens to the entire pipe infrastructure. The inspection task can be divided into two separate activities: an imaging task, demanded to a scope camera or similar, and a

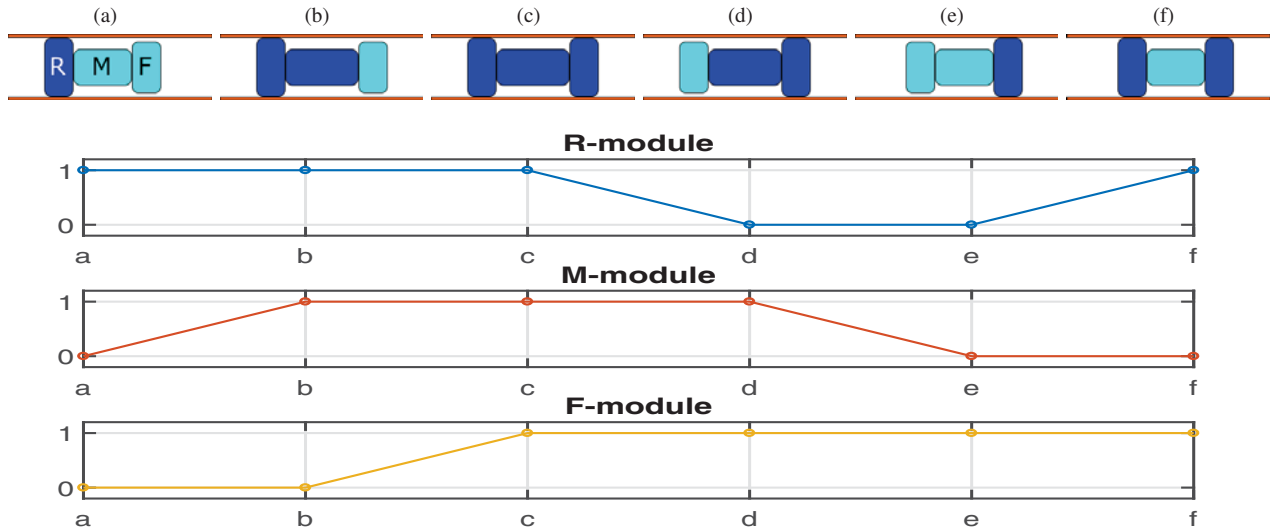


Fig. 8. Evolution of the three chambers in a forward gait cycle. Inflated chambers are dark blue (top rows) and 1 (bottom plots). Deflated chambers are light cyan (top rows) and 0 (bottom plots).

locomotion task, to effectively move the camera along the pipe. Inchworm robots represent an effective solution to this second task. In principle they can exploit different types of propulsion, but a very important constraint is that of avoiding risk of explosion in gas-saturated atmospheres (see e.g. ATEX international regulation [25]). A very simple way to comply to these norms is avoiding as much as possible electrical components, especially those with brushes - as DC electric motors. Because of this, there exist several attempted solutions to this problem that rely on pneumatic actuation from a remote air supply via a set of flexible pipes.

Inchworm robots substantially require two kinds of forces to implement propulsion: an impelling force and a holding force. The former is the force to push the robot forward, while the latter serves to fix the robot against the pipe wall. The right sequencing of these forces produces propulsion in a pipe. More precisely, an inchworm usually requires a set of at least three modules (see Fig. 8) to alternate their activation in the right order. Call “R” and “F” the rear and front modules of the worm, respectively, that have the function to hold the robot against the pipe walls, and call “M” - middle - the elongation module, responsible for the impelling movement. The forward gait cycle, in Fig. 8, consists of the six phases from (a) to (f). Playing the same cycle in reverse, on the other hand, will yield backward locomotion.

Usually, to enable the control of the three chambers, three separate air-pipes would be needed, in order to route air from the air supply, beyond the inspection hatch, to the robot. Moreover, also three valves are needed to control the pressure in the three chambers independently.

A. DESIGN

To make the system able to crawl forward and backward, we have a set of two desired behaviors. One of these two behaviors - forward crawling - is shown in Fig. 8-top. The other behavior is obtained by reversing the sequence. By

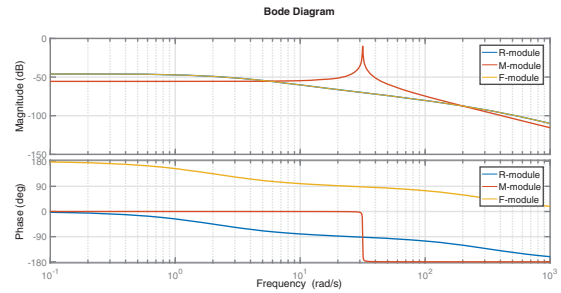


Fig. 9. Bode diagram for three out of phase mass-spring-damper systems. In the gain plot the blue (R-module) and yellow (F-module) lines overlap.

analyzing the modules evolution with respect to time (Fig. 8-bottom), it is possible to identify three equal waves with different phases. The phases in the two behaviors are in opposition. Since the desired motions are cyclic, the relative phase between the modules is more important than the absolute one. By modeling the chambers as simple mass-spring-damper systems, and by choosing suitable values for the mechanical parameters, their relative phases can be derived from the Bode diagram of their transfer functions. Fig. 9 shows the Bode diagram of the three subsystems. It is possible to notice that in the frequency range about 10 rad/s, there is a relative phase of about 180° between “F” and “R” and about 90° between each of them and “M”. This relationship reverses in the frequency range about 10² rad/s.

In other words, the response of the system can be inverted by simply tuning the frequency of the input source, and the worm can move forward or backward, consequently. The selected parameters are reported in Tab. II.

B. MECHANICS

Fig. 1 shows the CAD of the prototype, which is composed of three modules Front, Middle and Rear as depicted in Fig. 10. Each module shares similar mechanical components,

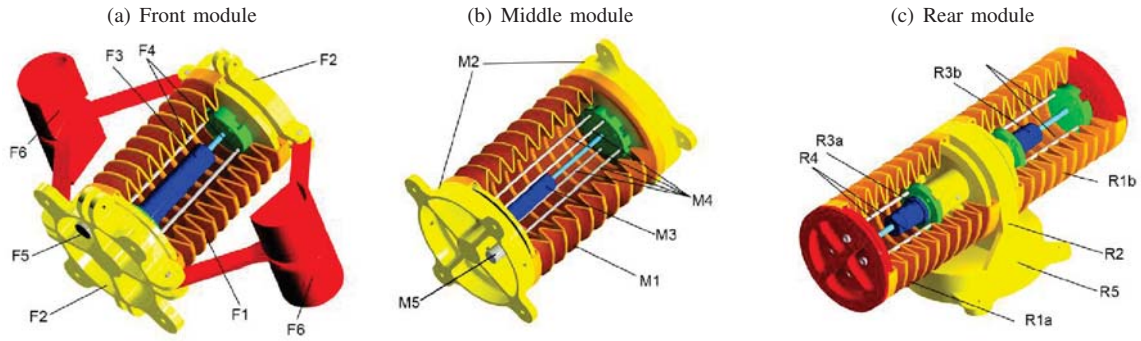


Fig. 10. 3D CAD renderings of the three modules that make up the inchworm

TABLE II
PARAMETERS OF THE SYSTEM

	module R	module M	module F
Mass [g]	300	300	350
Stiffness [N/m]	200	600	200
Damping Oil Viscosity [cP]	10^4	600	10^4

TABLE III
EXTENSIONS OF THE MODULES OF THE SYSTEM

	min length [mm]	max length [mm]
module R	147	183
module M	101	145
module F	97	141
inchworm	300	388

conveniently sized in order to match simulation results. Chambers are built using silicone modular bellows (F1, M1, R1), while collars and connecting components (F2, M2, R2) are 3D printed in ABS. Two different below sizes are employed, one size with external diameter of 60 mm for the front and rear chambers and one size of 83 mm for the central module, in order to have a longer gait. On the axis of each chamber a dashpot is placed (F3, M3, R3a, R3b)); different damping coefficients are obtained changing the oil viscosity. To implement suitable recoil forces, elastic bands (F4, M4, R4) are placed in parallel to the dashpot. By changing the number of bands assembled it is possible to regulate the module stiffness. Each module is provided with a pneumatic fitting (F5, M5, R5) to interface with the air pipe. The front and rear module are designed to expand transversely to the direction of motion and with opposite phases: when the pressure is such that the chamber inflates, the rear chamber expands while the front one shrinks. Rear module is realized with two bladders arranged perpendicularly to the central line of the system, while frontal module is equipped with a special mechanism (F6) composed by two beams hinged in the middle. The two others extremities of the beams are hinged to the collars. This configuration allows the beams to shrink when the pressure goes up and expand when the pressure goes down. Both front and rear module are equipped with soft Neoprene lattice pads in order to have higher friction and increase the surface in contact with the walls. Tab. III reports the minimum and maximum extensions of the three modules and of the entire worm.

V. EXPERIMENTAL VALIDATION

The air supply system relies on an external off-the-shelf air compressor attached to an electro-pneumatic regulator (model SMC ITV2030-31F2BN3-Q). A Custom electronic system with a ADC and DAC converters, is used to interface the pneumatic regulator to a Matlab/Simulink control scheme

TABLE IV

PARAMETERS OF THE EXPERIMENTS

condition	ω [rad/s]	P_0 [bar]	P_A [bar]
low freq.	0.5	0.02	0.07
high freq.	1.7	-0.02	0.15

(more details are available in [26]). Pressure can be regulated with a resolution of 0.025 Pa, at a sampling time of 0.01 s. During the experiment, the pressure is regulated following a reference in the form $P_r(t) = P_0 + P_A \sin(\omega t)$.

It is possible to regulate either the pressure bias P_0 and the pressure oscillation amplitude P_A and frequency ω . The value of $P(t)$ is intended with respect to the reference external (atmospheric in our case) pressure, and is saturated by it from below. When the reference pressure is set to 0 Pa the chambers deflate completely in about 5 seconds. Note, however, that this duration corresponds to the maximum deflation possible (from maximum inflated to completely deflated), a condition that is substantially far from the amount of deflation experienced during the presented experiments.

Two experiments are executed, corresponding to a high frequency and a low frequency excitations (see Fig. 11). The values of P_0 , P_A and ω for the two cases are reported in Tab. IV. A pipe mockup is used as environment. It includes two parallel boards 200 mm high, spaced 170 mm and placed on a flat surface. The experimental setup is video-recorded with a Canon HD camera and analyzed with the Kinovea software suite (see Fig. 12) [27].

Fig. 13 shows a series of screen-shots extracted from the two sessions, from which it is possible to appraise the two different strides executed by the system. Fig. 14 shows, for the two experimental conditions, the average x position of the system (panels a and b), and the effective inflation of the three chambers (panels c and d). These latter results shows how the phase differences between the chambers change

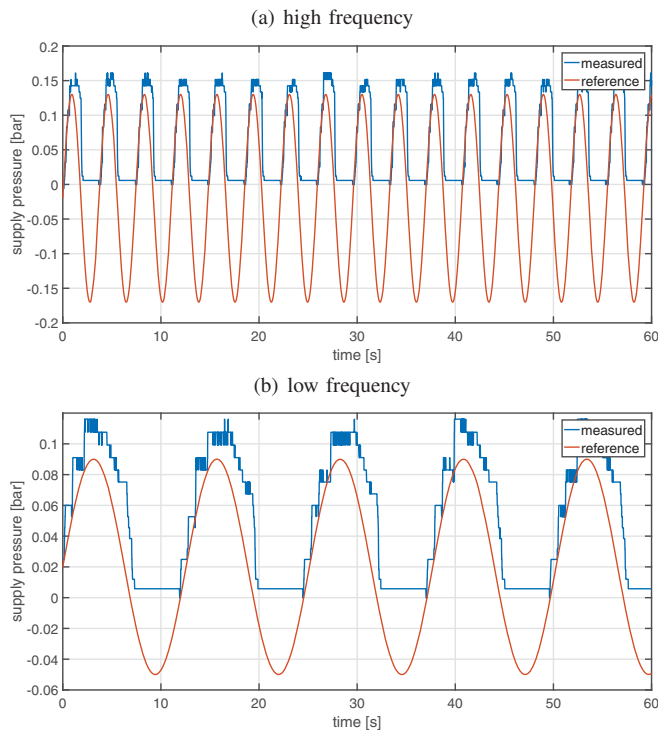


Fig. 11. Reference and measured supply pressure. Note that the measured pressure is saturated from below by the atmospheric pressure.



Fig. 12. Markers positions for the analysis in the Kinovea software suite.

across the two experimental conditions.

VI. DISCUSSION

Results from Fig. 14(a) and (b) show that the realized prototype is able to move forward and backward when suitable periodic profiles of pressure are applied to the device. The average speed reached by the prototype is 40 mm/min when moving forward and -20 mm/min, which is rather slow, still far from realistic application. Fig. 14(c) and (d) show the effective movement of the three modules during the two implemented strides.

Part of the system slowness is to be identified on the imperfect implementation of the three phases, which in turn can be adduced to model errors, as unmodeled frictions, imperfect knowledge of the damping implemented by the dashpot and of the stiffness of the springs. Another cause of the slowness can be attributed to the very principle of the mechanism. In fact, because of the relative phase among the

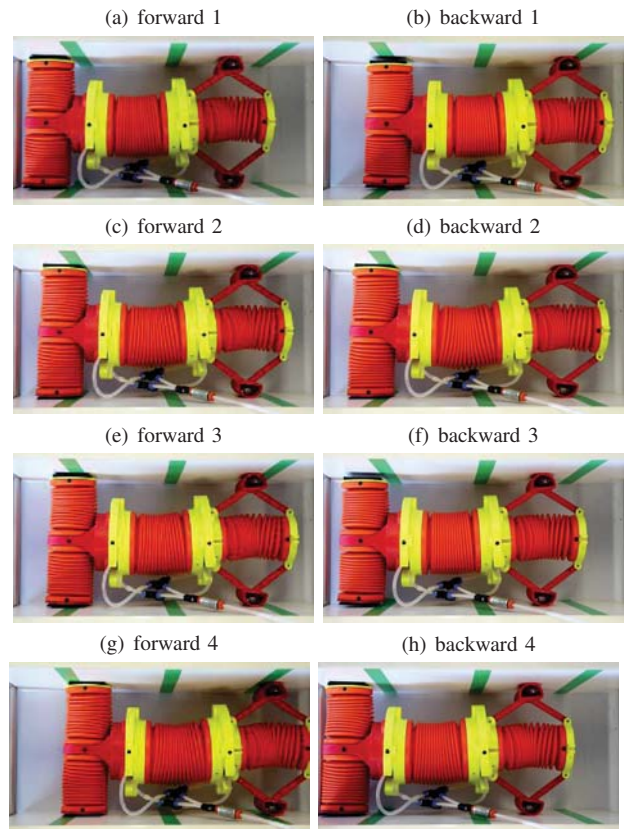


Fig. 13. Frames from the videos in which the inchworm moves forward (a,c,e,g) and backward (b,d,f,h)

chambers each gait always includes also a small contracting phase, so that the robot loses part of the covered distance. Looking at the results, this phase is larger when moving backward than when moving forward.

Despite the slow speed, we believe that these results are sufficient to prove the feasibility of the proposed approach, although showing space for improvement. For example, we believe that the system performances could be improved by using smaller chambers, because they would require a lower volume of air to be inflated.

VII. CONCLUSIONS

This paper presented a novel approach to the under-actuation of fluidic systems, based on the exploitation of the intrinsic mechanical properties of the system to obtain different dynamical responses, to reduce the number of pipes and valves to obtain a given family of desired behaviors. The principle was introduced in theory and explored in simulation. Afterward, the analysis of a case study - an inchworm robot for duct inspection - led to the implementation and experimental validation of the principle in a prototype. Results show the feasibility of the proposed approach, as well as opening several improvement opportunities in the technology, e.g. the integration of stiffness and damping in the chamber material to enable more compact realizations. In addition, it would be interesting to investigate the effects of some key parameters, e.g. the length of the feed line, onto

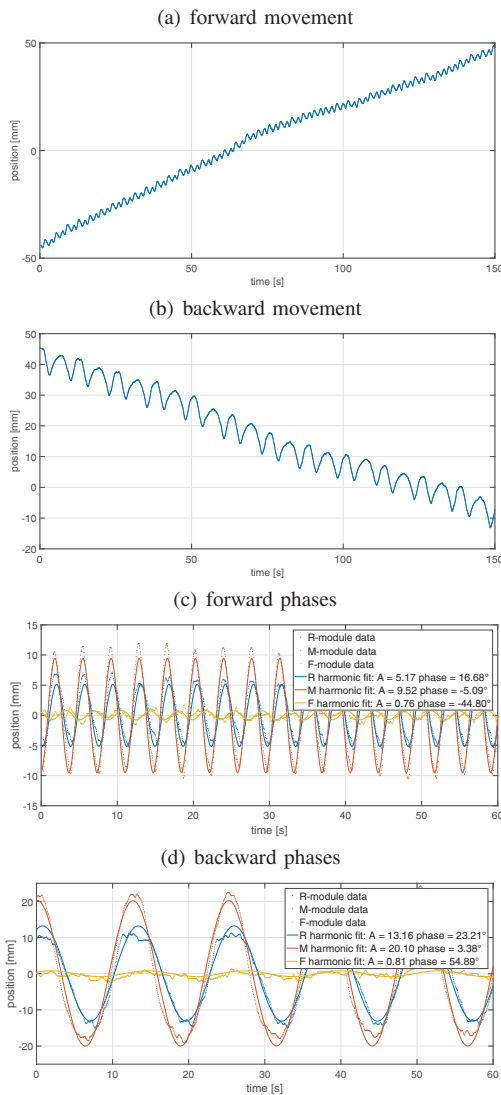


Fig. 14. Experimental results. Average x position of the system (panels (a) and (b)), and effective inflation of the chambers (panels (c) and (d)), for forward (left column) and backward (right column) movements. Raw data in panels (c) and (d) is flanked by a line fitting the data on a model of first order Fourier expansion ($y = A_0 + A \sin(\omega t + \phi)$), from where amplitude and phase are deduced. For legibility panels (c) and (d) show a shorter time frame than panels (a) and (b). Note that the blue sine wave corresponds to the longitudinal phase of the “F” module, not to the transverse one (the one shown in Fig. 9), w.r.t. which it is shifted by 180° .

the feasible frequency bandwidth.

ACKNOWLEDGMENT

The authors thank Andrea Di Basco and Gaspare Santaera for their help in the implementation of the prototype.

REFERENCES

- [1] D. Rus and M. T. Tolley, “Design, fabrication and control of soft robots,” *Nature*, vol. 521, no. 7553, p. 467, 2015.
- [2] C. Laschi, B. Mazzolai, and M. Cianchetti, “Soft robotics: Technologies and systems pushing the boundaries of robot abilities,” *Science Robotics*, vol. 1, no. 1, p. eaah3690, 2016.
- [3] B. Vanderborght, A. Albu-Schäffer, A. Bicchi, E. Burdet, D. G. Caldwell, R. Carloni, M. Catalano, O. Eiberger, W. Friedl, G. Ganesh *et al.*, “Variable impedance actuators: A review,” *Robotics and autonomous systems*, vol. 61, no. 12, pp. 1601–1614, 2013.

- [4] C. Semini, N. G. Tsagarakis, B. Vanderborght, Y. Yang, and D. G. Caldwell, “Hyq-hydraulically actuated quadruped robot: Hopping leg prototype,” in *Biomedical Robotics and Biomechanics, 2008. BioRob 2008. 2nd IEEE RAS & EMBS International Conference on*. IEEE, 2008, pp. 593–599.
- [5] J. M. Bern, G. Kumagai, and S. Coros, “Fabrication, modeling, and control of push robots,” in *Proceedings of the International Conference on Intelligent Robots and Systems*, 2017.
- [6] “Active protective — hip protection for older adults,” <http://activeprotective.com/>, (Accessed on 09/14/2017).
- [7] “Hvding the new bicycle helmet with an airbag,” <https://hovding.com/>, (Accessed on 09/14/2017).
- [8] “Mangar health — inflatable bath pillow, movement and transport aids,” <https://mangarhealth.com/>, (Accessed on 09/14/2017).
- [9] “Soft robotics,” <https://www.softroboticsinc.com/>, (Accessed on 09/14/2017).
- [10] “Corporate website — festo corporate,” <https://www.festo.com/>, (Accessed on 09/14/2017).
- [11] R. Deimel and O. Brock, “A novel type of compliant and underactuated robotic hand for dexterous grasping,” *The International Journal of Robotics Research*, vol. 35, no. 1-3, pp. 161–185, 2016.
- [12] A. J. Ijspeert, A. Crespi, D. Ryzcko, and J.-M. Cabelguen, “From swimming to walking with a salamander robot driven by a spinal cord model,” *science*, vol. 315, no. 5817, pp. 1416–1420, 2007.
- [13] A. D. Marchese, C. D. Onal, and D. Rus, “Autonomous soft robotic fish capable of escape maneuvers using fluidic elastomer actuators,” *Soft Robotics*, vol. 1, no. 1, pp. 75–87, 2014.
- [14] R. F. Shepherd, F. Ilievski, W. Choi, S. A. Morin, A. A. Stokes, A. D. Mazzeo, X. Chen, M. Wang, and G. M. Whitesides, “Multigait soft robot,” *Proceedings of the National Academy of Sciences*, vol. 108, no. 51, pp. 20 400–20 403, 2011.
- [15] C. D. Onal and D. Rus, “Autonomous undulatory serpentine locomotion utilizing body dynamics of a fluidic soft robot,” *Bioinspiration & biomimetics*, vol. 8, no. 2, p. 026003, 2013.
- [16] A. M. Bertetto and M. Ruggiu, “In-pipe inch-worm pneumatic flexible robot,” in *Advanced Intelligent Mechatronics, 2001. Proceedings. 2001 IEEE/ASME International Conference on*, vol. 2. IEEE, 2001, pp. 1226–1231.
- [17] M. Hussein, “Modelling and control of a worm-like micro robot with active force control capability,” 2010.
- [18] A. A. Gargade and S. S. Ohol, “Development of in-pipe inspection robot.”
- [19] R. F. Shepherd, F. Ilievski, W. Choi, S. A. Morin, A. A. Stokes, A. D. Mazzeo, X. Chen, M. Wang, and G. M. Whitesides, “Multigait soft robot,” *Proceedings of the National Academy of Sciences*, vol. 108, no. 51, pp. 20 400–20 403, 2011.
- [20] N. Napp, B. Araki, M. T. Tolley, R. Nagpal, and R. J. Wood, “Simple passive valves for addressable pneumatic actuation,” in *Robotics and Automation (ICRA), 2014 IEEE International Conference on*. IEEE, 2014, pp. 1440–1445.
- [21] J. Lim, H. Park, J. An, Y.-S. Hong, B. Kim, and B.-J. Yi, “One pneumatic line based inchworm-like micro robot for half-inch pipe inspection,” *Mechatronics*, vol. 18, no. 7, pp. 315–322, 2008.
- [22] M. Wehner, R. L. Truby, D. J. Fitzgerald, B. Mosadegh, G. M. Whitesides, J. A. Lewis, and R. J. Wood, “An integrated design and fabrication strategy for entirely soft, autonomous robots,” *Nature*, vol. 536, no. 7617, p. 451, 2016.
- [23] C. Piazza, C. Della Santina, M. Catalano, G. Grioli, M. Garabini, and A. Bicchi, “Soft-hand pro-d: Matching dynamic content of natural user commands with hand embodiment for enhanced prosthesis control,” in *Robotics and Automation (ICRA), 2016 IEEE International Conference on*. IEEE, 2016, pp. 3516–3523.
- [24] F. M. White, “Fluid mechanics, web,” *Ed McGraw-Hill Boston*, 1999.
- [25] “Equipment for potentially explosive atmospheres (atex) - european commission,” https://ec.europa.eu/growth/sectors/mechanical-engineering/atex_en, (Accessed on 09/14/2017).
- [26] C. Della Santina, C. Piazza, G. M. Gasparri, M. Bonilla, M. G. Catalano, G. Grioli, M. Garabini, and A. Bicchi, “The quest for natural machine motion: An open platform to fast-prototyping articulated soft robots,” *IEEE Robotics & Automation Magazine*, vol. 24, no. 1, pp. 48–56, 2017.
- [27] J. Charmant and contributors, “Kinovea,” 2016. [Online]. Available: <http://www.kinovea.org>